Article

Inversion Method of Tidal Level Based on GNSS Triple-Frequency, Geometry-Free, Non-Ionospheric Phase Combination

Gaochong You [1], **Hang Guo** [1], **Jianfeng Wu** [1] and **Min Yu** [2,*]

[1] School of Information Engineering, Nanchang University, Nanchang 330031, China; ygc946066110@gmail.com (G.Y.); guo1_2002@hotmail.com (H.G.); wjf19970805@163.com (J.W.)
[2] College of Software, Jiangxi Normal University, Nanchang 330022, China
* Correspondence: myu@jxnu.edu.cn

Abstract: Using the navigation signal transmitted by GNSS (global navigation satellite system), satellites for tide level monitoring comprise one of the important research fields of GNSS marine remote sensing. Regarding the problem that GNSS-MR (multipath reflectometry) technology only uses carrier SNR (signal noise ratio) data, resulting in the lack of SNR data for early CORS (continuously operating reference stations) stations, it is impossible to carry out tide level inversion. In this paper, a method of tide level inversion based on triple-frequency geometric ionospheric free combined-phase observations instead of SNR is proposed. The simultaneous interpretation of GNSS satellite observations from the sc02 station in Friday Harbor in the US is carried out and compared with the traditional GNSS-IR (interference and reflectometry) tide-inversion method. The experimental results show that the tide level inversion method proposed in this paper has the same tide level trend as the measured tide level trend. The accuracy evaluation shows that the RMSE value of tide level inversion is 15 cm and the correlation coefficient r is 0.984, which verifies the effectiveness of this method for tide level monitoring and expands the method of GNSS tide-level monitoring.

Keywords: global navigation satellite system; tide level monitoring; multipath effect; GNSS-MR; triple-frequency; geometry-free; ionospheric phase combination

1. Introduction

The GNSS (global navigation satellite system) was originally designed to provide users with positioning (P), velocity measurement (V), timing (T), and other services. In the positioning process, it is affected by the reflected signal of the surrounding environment, resulting in the carrier-phase value estimated by the receiver deviates from the real value, and the positioning accuracy has never been reduced, which is the multipath effect of the global positioning system. With the deepening of GNSS research, surface remote sensing monitoring technology based on the GNSS multipath effect, GNSS-MR (GNSS multipath reflectometry) technology, has been developed internationally. At present, this technology has been widely studied in soil moisture inversion [1], deep monitoring [2], reservoir and river water level monitoring [3], and marine tide level monitoring [4].

The classical GNSS-MR theory uses the signal-to-noise ratio of the navigation satellite in the low-altitude area, removes the trend through quadratic fitting, extracts the frequency value of the periodic term through the Lomb–Scargle spectrum analysis method, and then obtains the effective inversion height from the antenna phase center to the sea surface. In reference [5], the airborne receiver is used to receive the sea-surface reflection signal for sea-surface height inversion, and the RMSE (root mean square error) of airborne GNSS-R tide level monitoring is 10 cm. GNSS-R technology requires the erection of two antennas, which increases the equipment cost. In view of this, the authors of [6,7] have been carried out the research on the multi-path value and measured carrier signal-to-noise ratio of the

receiver; a physical model for height measurement using SNR, that is, classical GNSS-MR technology, has been proposed; and this method has been used to study snow-depth monitoring. Subsequently, the authors of [8–10] carried out inversion research on soil humidity, snow-depth change, and ocean tide level and developed corresponding GNSS-MR software. In view of the fact that GNSS-MR technology only uses SNR data, when using GNSS for snow-depth monitoring, the authors of [11] proposed a method of snow-depth inversion with an L4 signal without geometric distance. Due to the interference of the ionosphere, the inversion accuracy of this method is low. In reference [12], to tackle the poor accuracy of snow-depth inversion caused by ionospheric interference in the L4 method, a triple-frequency snow-depth inversion method without geometric distance and ionospheric phase combination is proposed and compared with the classical GNSS-MR method, and the same classical experimental results are obtained.

At present, the research on tide level inversion using gnss-mr technology is based on navigation signal signal-to-noise ratio data, and there is a lack of tide level inversion research using more abundant navigation signal carrier-phase observations. Moreover, for early CORS stations, some GNSS receivers do not provide navigation signal-to-noise ratio data. Therefore, carrying out tide level inversion using carrier-phase observations can better enhance the universality of GNSS tide level monitoring. Based on the above problems, this paper carries out the research work of tide level inversion based on triple-frequency combined-phase observations, so as to provide a new method for GNSS tide level inversion.

2. The Basic Principle of Tidal Inversion

2.1. Multipath Signal and Carrier-Phase Offset

Affected by the sea-surface multipath effect, the sea-surface reflected signal causes the measured carrier signal-to-noise ratio of the receiver to produce periodic oscillation in the low-altitude angle region of the satellite. It also makes the measured carrier-phase value produce a small (millimeter level) periodic variation of carrier measurement offset; the frequency of signal-to-noise ratio periodic term and the periodic variation frequency of carrier measurement offset are related to the height variation between the antenna phase center and the sea surface. The former is the theoretical basis of classical GNSS-MR tide level inversion, and the latter is the theoretical basis of this method.

Figure 1 shows the basic model of tide level inversion of the shore-based receiver. In the figure, H represents the height from the antenna phase center to the reflecting surface, also known as the effective inversion height; h is the vertical height from the celestial center phase center to the datum of the tide gauge station; and θ represents the altitude angle of the satellite.
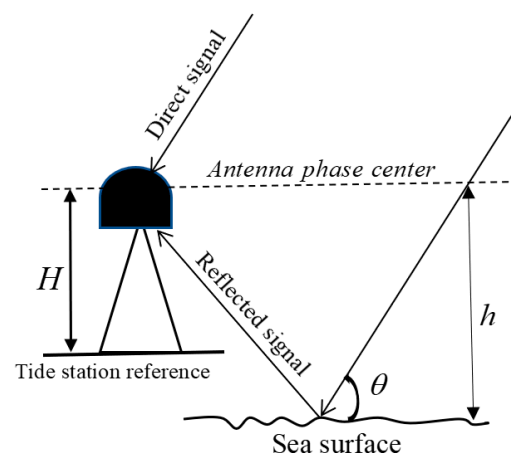

Figure 1. The tidal-level inversion model.

The amount of phase delay generated by the reflected signal received by the receiver compared with the direct signal satisfies the following relationship:

$$\delta\varphi = \frac{4\pi h}{\lambda}\sin\theta \tag{1}$$

where h is the height from the antenna phase center to the sea surface, λ is the carrier wavelength, and θ is the satellite altitude angle.

The direct signal of satellite S_d can be simplified as the following formula:

$$S_d = Ap(t)\sin(2\pi ft) \tag{2}$$

where A is the signal amplitude, of which $p(t)$ is the exclusive or sum of ± 1 data code and pseudo code, f is the carrier frequency, and the reflected signal of the direct satellite direct is

$$S_m = \alpha Ap(t-\tau)\sin(2\pi f(t-\tau)+\delta\varphi) \tag{3}$$

where α is the reflection coefficient, t is time variable, τ is the propagation time delay, and $\delta\varphi$ is the phase delay represented by Equation (1). The satellite signal actually received by the receiver can be expressed as

$$S(t) = Ap(t)\sin(2\pi ft)+\alpha Ap(t-\tau)\sin(2\pi f(t-\tau)+\delta\varphi) \tag{4}$$

When $S(t)$ performs a correlation operation with the copied C/A code inside the receiver, the phase deviation θ_e of the detected synthetic signal compared with the direct signal satisfies the following equation [13]:

$$\theta_e = \arctan\left(\frac{\alpha R(t-\tau)\sin\delta\varphi}{R(t)+\alpha R(t-\tau)\cos\delta\varphi}\right) \tag{5}$$

$R(t)$ is the autocorrelation function of C/A. If the difference between $R(t-\tau)$ and $R(t)$ is ignored, the above formula can be simplified as

$$\theta_e = \arctan\left(\frac{\sin\delta\varphi}{\alpha^{-1}+\cos\delta\varphi}\right) \tag{6}$$

Affected by the fact that the receiver antenna can only receive right-handed circular polarity signals, $\alpha \ll 1$. Therefore, the above formula can be further simplified to the following equation:

$$\theta_e = \alpha\sin\delta\varphi = \alpha\sin(\frac{4\pi h}{\lambda}\sin\theta) \tag{7}$$

It can be seen from Equation (7) that the carrier-phase offset changes periodically with the sinusoidal value of the satellite altitude angle, and the frequency is related to the wavelength of the satellite signal and the height from the antenna phase center to the sea surface. Because the carrier-phase offset is difficult to directly separate from the carrier-phase offset, the triple-frequency combined-phase observation resolution carrier-phase offset is used in this paper.

2.2. Triple-Frequency, No Geometry, and No Ionosphere Combination

The triple-frequency combined-phase observation is defined as the linear combination of the carrier-phase deviation of three bands [12]:

$$M_{1,2,5}(t) = (\lambda_5^2(\lambda_1\widetilde{\phi}_1(t)-\lambda_2\widetilde{\phi}_2(t))+\lambda_1^2(\lambda_2\widetilde{\phi}_2(t)-\lambda_5\widetilde{\phi}_5(t)) \\ +\lambda_2^2(\lambda_5\widetilde{\phi}_5(t)-\lambda_1\widetilde{\phi}_1(t)))/(1\text{m}^2) \tag{8}$$

where $\lambda_1 = 0.1902937$ m, $\lambda_2 = 0.2442102$ m, and $\lambda_5 = 0.2548280$ m represent the wavelengths of L1, L2, and L5 carriers of GPS, respectively. $\widetilde{\phi}_i$ represents the sum of the

superimposed value of the carrier-phase value of the direct signal and the carrier-phase offset of the multipath reflected signal, which satisfies the following equation:

$$\widetilde{\phi}_i = \varphi_i(t) + \beta_i(t) \tag{9}$$

where, the following table represents specific band signals. In this paper, assuming that the antenna gains of three different frequencies are exactly the same, Equation (8) can be further written as the following equation:

$$M_{1,2,5}(t) = k_1 \widetilde{\phi}_1 + k_2 \widetilde{\phi}_2 + k_5 \widetilde{\phi}_5 \tag{10}$$

where

$$
\begin{aligned}
\widetilde{\phi}_i(t) &= 2\pi\varphi_i(t) + \beta_i(t) \\
k_1 &= \lambda_1\eta_1, k_2 = \lambda_2\eta_2, k_5 = \lambda_5\eta_5 \\
\eta_1 &= \frac{(\lambda_5^2 - \lambda_2^2)}{1m^2}, \eta_2 = \frac{(\lambda_1^2 - \lambda_5^2)}{1m^2}, \eta_1 = \frac{(\lambda_2^2 - \lambda_1^2)}{1m^2} \\
u &= k_1 N_1 + k_2 N_2 + k_5 N_5
\end{aligned} \tag{11}
$$

After the linear combination of the three carrier-phase observations of GPS, the linear distance between the satellite and the receiver, the ionospheric delay, and the convective layer delay is effectively eliminated. Since the combination amount U of ambiguity has no effect on the periodicity of the carrier-phase offset, the triple-frequency combined-phase observations can be regarded as the linear combination of the carrier-phase offset of the triple-frequency bands, and Equation (10) can be further written as the following equation:

$$M_{1,2,5}(t) = k_1 \beta_1(t) + k_2 \beta_2(t) + k_5 \beta(t)_5 \tag{12}$$

The effective wavelength of the combined phase is

$$\lambda_{1,2,5} = \left(\frac{\eta_1}{\lambda_1} + \frac{\eta_2}{\lambda_2} + \frac{\eta_5}{\lambda_5} \right)^{-1} = 465.005 \text{ m} \tag{13}$$

Like the classical GNSS-MR tide level inversion principle, the frequency of the triple-frequency combined-phase observation value that varyies with the sinusoidal value of the height angle is linear with the effective inversion height. The difference is that the tide level height value needs to be observed in advance for a period of time to establish a linear model between the effective inversion height and the triple-frequency combined-phase observation value.

The sinusoidal value of the height angle is a variable with unequal spacing, so it is impossible to extract the frequency information from the triple-frequency carrier-phase combination observation value by fast Fourier transform. Therefore, the Lomb–Scargle spectrum method is used to extract the frequency value of the combined signal in this paper. The algorithm is as follows [13,14]:

$$P_x(f) = \frac{1}{2\delta^2} \left\{ \frac{\left[\sum (\phi_n'^j - \overline{\phi'^j}) \cos \omega(t_n - \tau) \right]^2}{\sum \cos^2 \omega(t_n - \tau)} + \frac{\left[\sum (\phi_n'^j - \overline{\phi'^j}) \sin \omega(t_n - \tau) \right]^2}{\sum \sin^2 \omega(t_n - \tau)} \right\} \tag{14}$$

where $\overline{\phi'^j}$ and δ^2 are the mean and the variance of the triple-frequency combined-phase observations, respectively, and ω is the angular frequency.

3. Example Analysis

In this paper, the satellite observation data of the sc02 station in Friday Harbor Port, Washington, USA are selected for experimental verification. The sc02 station is subordinate to the plate edge observation PBO network of the "earth scope" of the United States. It is built near the sea and equipped with a Trimble netr9 geodetic receiver. It can accept the sea-surface reflection signal in the sea-surface direction at the direction angle of 45°~220°.

The height h of the antenna phase center is 5.389 m. A tide-gauge station is built near the station, which can provide tide level data once every 6 min. Figure 2 shows the surrounding environment of the sc02 station, and Figure 3 shows the geographical location of the sc02 station. It is said that under the influence of the gravitational pull of the moon and the sun, the sea-surface height changes periodically with the occurrence of the sea-surface height, and the sea-surface change period with time is about one month, so when the technology is used to achieve one-month tide level inversion, it can explain the effectiveness of the technology for a long time. Therefore, this paper uses one month's GPS satellite observation data from Friday Harbor sc02 station from 1 August to 31 August 2020 for the experiments.

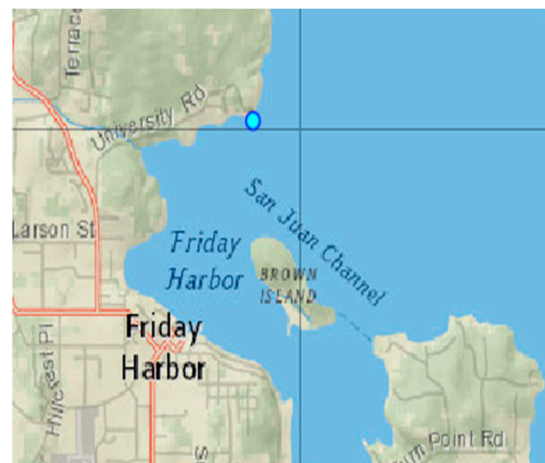**Figure 2.** The ssc02 station's surrounding environment.

Figure 3. The geographical location of the sc02 station.

3.1. Model Establishment

By observing the satellite carrier-phase data and the sea-surface height change for a period of time, a primary model between the triple-frequency combined-phase observation value for tide level monitoring and the effective inversion height is established. Figure 4 shows the periodic diagram (Figure 4a) of the observed value of the triple-frequency combined phase in the low-altitude angle area of a typical GPS satellite varying with the satellite altitude angle and the corresponding Lomb–Scargle spectrum (Figure 4b). It can be seen from Figure 4a that the observed value of the triple-frequency combined phase changes periodically with the change of satellite height, and the oscillation amplitude changes between −0.5 and 0.5. The abscissa corresponding to the peak in Figure 4b is the estimated frequency value of the combined phase, and the frequency value of the combined phase is 37.07 Hz.
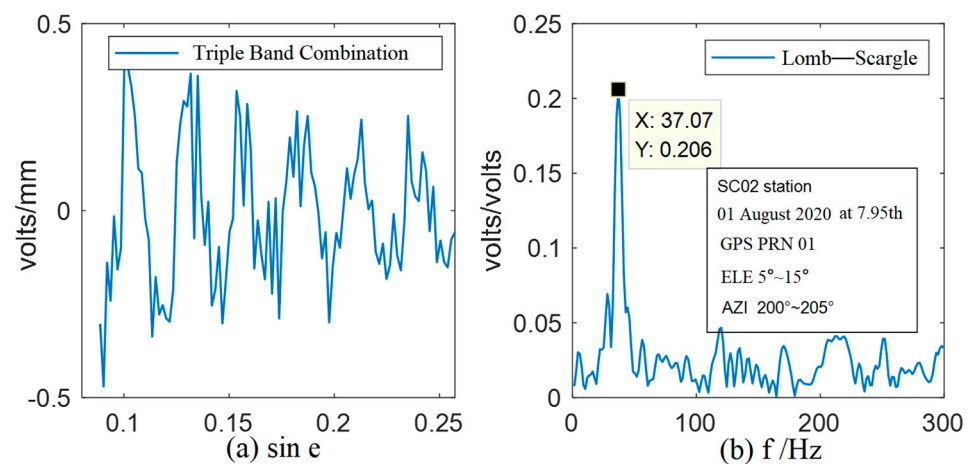
Figure 4. Periodic diagram (**a**) The triple-frequency combined-phase observation and (**b**) the Lomb-Scargle spectrum; sin *e* is the sinusoidal value of the satellite altitude angle *e*.

The tide level inversion model is established based on the satellite observation data and the tide level data for 15 consecutive days from 1 August 2020 to 15 August 2020. The effective inversion height h is calculated by subtracting the tide level height solution from the height *h* of the antenna phase center. Through the spectrum analysis of the triple-frequency combined-phase observation values, the frequency *f* is obtained, and then the primary model of the effective reflection height and frequency *f* is established.

Figure 5 shows a model between the height from the antenna phase center to the reflecting surface and the frequency of the combined phase observation which is obtained by Lomb-scargle spectrum analysis method. The relationship between them is obtained by the least square method in the sc02 station. It is a linear relationship. According to the least square fitting, the antenna height *h* from the sea surface (the reflecting surface) and the *f* constitute the following linear relationship:
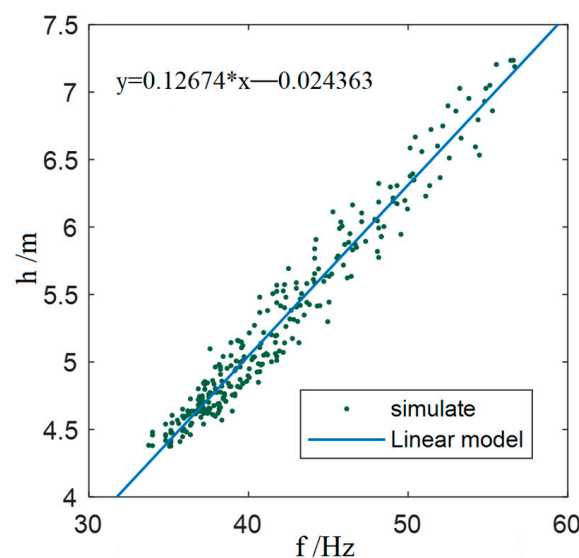
$$h = 0.12674f - 0.024363 \tag{15}$$

Figure 5. The linear relationship diagram between the antenna phase center and the peak frequency of the Lomb–Scargle spectrum analysis. The longitudinal ordinate *h* represents the height from the antenna phase center to the reflective surface; the horizontal ordinate *f* represents the peak frequency corresponding to the Lomb–Scargle spectrum.

3.2. Using the Model to Retrieve Tidal Level

According to the model established in Section 2.1, when the frequency value of the triple-frequency combined-phase observation value of the satellite in the sea-surface reflection area is determined, the effective inversion height h can be obtained from Formula (15), and then the sea-surface height h_r can be obtained from antenna height h and $h_r = H - h$.

Based on the above basic theory and the tide level inversion model, the tide level of the sc02 station on 16 August and 31 August 2020 in the Friday Harbor port is inversed in this paper. In order to facilitate simultaneous interpreting with the traditional GNSS-MR tidal-level inversion method [15], a comparison is made. At the same time, GNSS-MR technology is used to retrieve the tide level of the Friday Harbor port. The results are shown in Figure 6. In the figure, the solid line is the measured tide level change curve of the tide-gauge station, the brown scattered point is the tide level value retrieved by the GNSS-MR technology, and the green scattered point is the tide level value retrieved by the algorithm in this paper. The tidal dispersion retrieved by this algorithm changes periodically with the change of the tidal level height, which shows that this method can monitor the tidal level and the GNSS-MR technology.
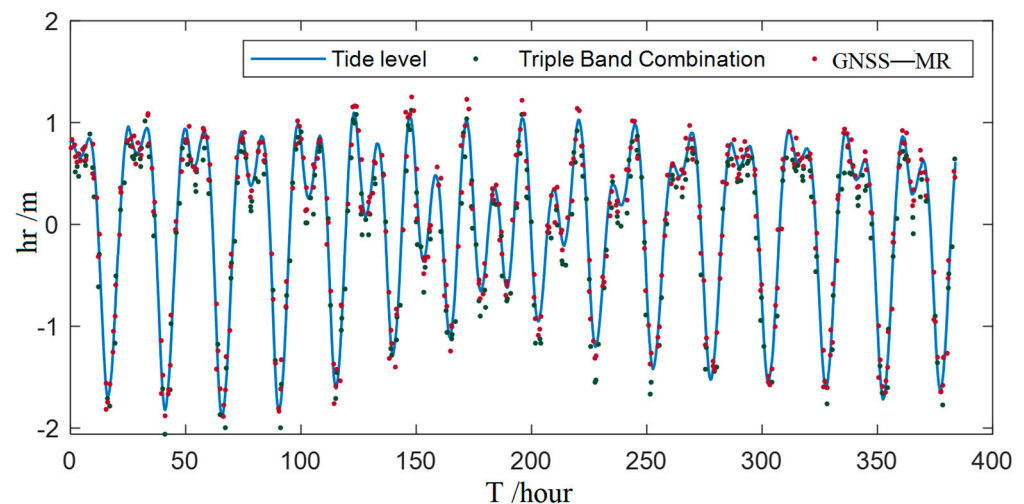

Figure 6. The tide level inversion method of the triple-frequency combined-phase observations, the tidal-level inversion results of the GNSS-MR technology, and the measured tide level change curve. The vertical axis h_r represents the tide height; the horizontal axis T indicates the inversion time.

By subtracting the measured tidal level from the inversion value, the inverse tidal level deviation scatter map can be obtained in Figure 7, where the horizontal axis represents the time in hours, while the vertical axis represents the inversion deviation value in meters. The brown scatter points represent the tide level inversion deviation results of the GNSS-MR technology, and the green scatter points represent the tide level inversion deviation results of this algorithm. It can be seen that the deviation values of the tide level inversion of the GNSS-MR technology and this algorithm are −0.5~0.5 m. Figure 8 further shows these two methods. It can be seen from the figure that the deviation of the tide level retrieved by these two methods is normally distributed, and it is the influence of the noise interference.

The Figure 8 is the histogram of the statistical distribution of the tidal deviation of two methods, which are the triple-frequency combined inversion of the tide level method (a) and the GNSS-MR inversion (b).

The Figure 9 analyzed the results and obtained the relationship among the height of GNSS-MR tide level inversion method, the height of triple-frequency combined method, and the tide level height. The longitudinal axis h_r indicates the tide level height of the inversions; the horizontal axis h indicates the measured tide level height of the tide gauge station in the Figure 9.
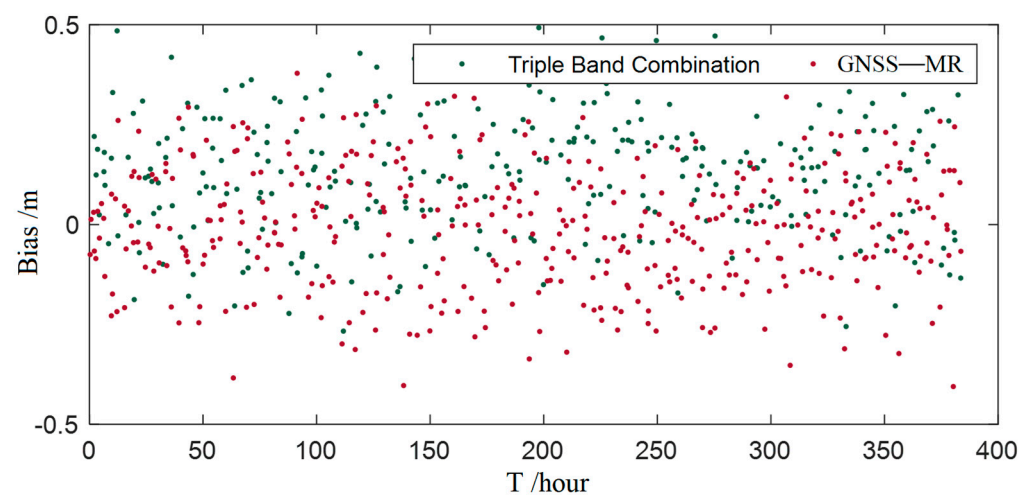
Figure 7. The inversion of the tide level by the triple-frequency combined tidal tide-inversion method and GNSS-MR, respectively. Bias represents the difference between the inversion tide point value and the measured tide point value of the tide detector; the abscissa T indicates the time of the tide level inversion.
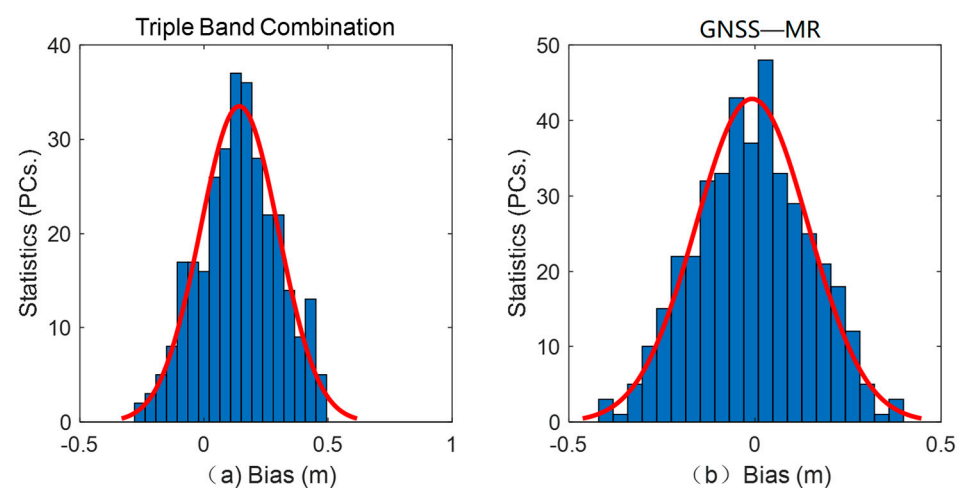

Figure 8. The histogram of the statistical distribution of the tidal deviation of (**a**) triple-frequency combined inversion of the tide level method and (**b**) the GNSS-MR inversion.
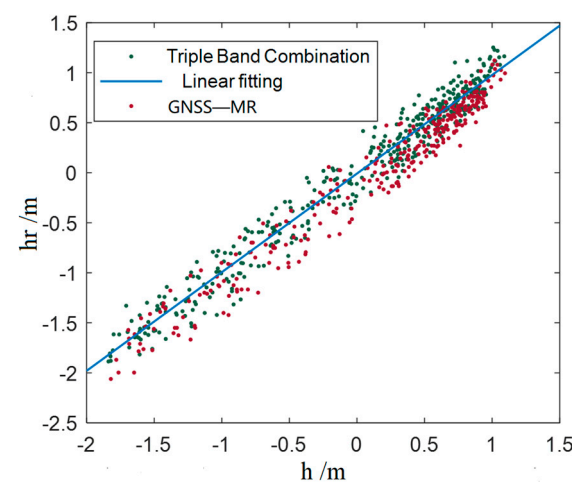

Figure 9. The relationship between the height of the GNSS-MR tide level inversion method/triple-frequency combined method and the tide level height of the tide gauge station.

In this paper, root mean square RMSE and correlation coefficient *r* are used as the evaluation criteria for the accuracy of the tide level inversion, and the accuracy of the triple-frequency combined-phase observation tide level inversion method and the GNSS-MR tide level inversion method are evaluated, respectively. The results are shown in Table 1. The RMSE value of the inversion tide level of the triple-frequency combined-phase tide level inversion method is 16.2 cm, and the correlation coefficient with the measured tide level is 0.977. The RMSE value of the GNSS-MR tide level inversion is 15.7 cm, and the correlation coefficient with the measured tide level is 0.981. It can be seen that the inversion accuracy and the correlation coefficient of the triple-frequency combined-phase tide level inversion method are approximately the same as those of the GNSS-MR tide level inversion method, which further proves the effectiveness of the triple-frequency combined-phase inversion tide level method.

Table 1. A comparison table of the inversion results.

Method	RMSE/m	Bias/m	Correlation Coefficient R	Inversion Points
Triple-frequency combination	0.162	0.005	0.977	309
GNSS-MR	0.157	−0.008	0.981	418

4. Conclusions

With the continuous development of global positioning systems and the deepening of research, ground-based remote sensing monitoring using navigation satellite signals has become one of the most important research hotspots, of which tide level monitoring is an important part. For the current tide level inversion, GNSS-MR technology based on a signal-to-noise ratio is mostly used; the signal-to-noise ratio data are not necessary for navigation and positioning, and some receivers do not provide them. To solve this problem, this paper proposes a method of inversion of the triple-frequency band of simultaneous interpreting without the tidal geometry and ionosphere. The data are measured by the observation data of the sc02 station in Friday Harbor of the United States and compared with the traditional GNSS-MR technology tide-inversion method.

Affected by the gravity of the sun and the moon, the tide level changes periodically with time. In this paper, the three carrier-phase observations of GPS L1, L2, and L5 observed by the sc02 station of Friday Harbor in the United States are linearly combined to eliminate the geometric distance and ionization measurement delay between the satellite and the receiver. The spectrum of the combined observations is analyzed to obtain the frequency value of the combined observations varying with the satellite height. The height from the phase center of different antennas to the reflector and the combined-phase frequency value are modeled once. Finally, the tide level inversion is carried out by using the combined-phase observation value and the primary model of the frequency from the antenna phase center to the reflector that is higher than the combined phase. The experimental results show that with the periodic fluctuation of the tide level, the tide level retrieved by this method can correspondingly respond, and the change trend of the retrieved tide level is the same as that measured by the tide-gauge station near Friday Harbor, which proves the effectiveness of this method. In order to evaluate the performance of the tide level inversion method in this paper, three performance indexes—RMSE, correlation coefficient R, and the number of successful inversions of the tide level—are used to evaluate the performance of the inversion results. The results show that the RMSE value of the tide level inversion method in this paper is 16.2 cm, the correlation coefficient r of the measured tide level at the same tide station is 0.977, and the total number of successful inversions of the tide level is 309. In order to further analyze the performance of this method in retrieving the tide level, this paper also uses the traditional gnss-mr technology and the observation data in the same time period to retrieve the tide level, which is compared with this method. The accuracy of traditional gnss-mr tide level inversion is 15.7 cm, the correlation coefficient is 0.981, and the total number of the retrieved tide levels is 418. The accuracy and correlation

coefficient of this method are slightly lower than that of the traditional gnss-mr tide level inversion method. The reason is that the vibration amplitude of the combined-phase observation value is at the millimeter level and can be easily disturbed by noise. The vibration amplitude of the SNR data used for gnss-mr is usually between 10 dB and 40 dB, which has stronger anti-interference. Therefore, the traditional method is slightly better than the method in this paper, but the inversion accuracy and the correlation coefficient are similar. The reason why the number of tide levels successfully retrieved by this method is less than that of the traditional method is that this method must require the satellite to broadcast more than three carrier signals. For early satellites, L5 carrier signals are not transmitted, but this has never led to the reduction of the number of inversions. Although the inversion performance of this method is slightly worse than that of the traditional gnss-mr method, considering that this method is aims to solve the problem that the tide level inversion cannot be carried out when the receiver does not provide SNR data, this method still has certain practical application value.

Author Contributions: Conceptualization, G.Y. and H.G.; methodology, G.Y.; software, G.Y.; validation, M.Y., H.G. and J.W.; formal analysis, G.Y.; investigation, G.Y.; resources, M.Y.; data curation, H.G.; writing—original draft preparation, G.Y.; writing—review and editing, H.G.; visualization, M.Y.; supervision, H.G.; project administration, M.Y.; funding acquisition, H.G. All authors have read and agreed to the published version of the manuscript.

Institutional Review Board Statement: Not applicable.

Informed Consent Statement: Not applicable.

Data Availability Statement: Not applicable.

Conflicts of Interest: The authors declare no conflict of interest.

References

1. Sun, B.; Liang, Y.; Han, M.; Yang, L.; Jing, L.; Hong, L. GNSS-IR soil moisture inversion method based on GA-SVM. *J. Beijing Univ. Aeronaut. Astronaut.* **2019**, *45*, 486–492.
2. Zhang, S.C.; Dai, K.N.; Nan, Y. Preliminary research on GNSS-MR for snow depth. *Geomat. Inf. Sci. Wuhan Univ.* **2016**, *43*, 11.
3. Lu, Z.; Feng, W.; Huang, D.F. Inversion of dam water level change by GNSS SNR signal. *Geod. Geodyn.* **2020**, *40*, 146–151.
4. Zhang, S.; Nan, Y.; Li, Z.; Zhang, Q.; Dai, K.; Zhao, Y. Analysis of tide variation monitored by GNSS-MR. *Acta Geod. Cartogr. Sin.* **2016**, *45*, 1042–1049.
5. Ruffini, N.G.; Soulat, F.; Caparrini, M.; Germain, O.; Martín-Neira, M. The Eddy Experiment: Accurate GNSS-R ocean altimetry from low altitude aircraft. *Geophys. Res. Lett.* **2004**, *31*, 261–268. [CrossRef]
6. Bilich, A.; Larson, K.M. Correction published 29 March 2008: Mapping the GPS multipath environment using the signal-to-noise ratio (SNR). *Radio Sci.* **2007**, *42*, 1–16.
7. Bilich, A.; Larson, K.M.; Axelrad, P. Modeling GPS phase multipath with SNR: Case study from the Salar de Uyuni, Boliva. *J. Geophys. Res. Solid Earth* **2008**, *113*, B4. [CrossRef]
8. Shi, Y.; Ren, C.; Yan, Z.; Lai, J. High Spatial-Temporal Resolution Estimation of Ground-Based Global Navigation Satellite System Interferometric Reflectometry (GNSS-IR) Soil Moisture Using the Genetic Algorithm Back Propagation (GA-BP) Neural Network. *ISPRS Int. J. Geo-Inf.* **2021**, *10*, 623. [CrossRef]
9. Tabibi, S.; Geremia-Nievinski, F.; van Dam, T. Statistical comparison and combination of GPS, GLONASS, and multi-GNSS multipath reflectometry applied to snow depth retrieval. *IEEE Trans. Geosci. Remote Sens.* **2017**, *55*, 3773–3785. [CrossRef]
10. Roesler, C.; Larson, K.M. Software tools for GNSS interferometric reflectometry (GNSS-IR). *GPS Solut.* **2018**, *22*, 10. [CrossRef]
11. Ozeki, M.; Heki, K. GPS snow depth meter with geometry-free linear combinations of carrier phases. *J. Geod.* **2012**, *86*, 209–219. [CrossRef]
12. Yu, K.; Ban, W.; Zhang, X.; Yu, X. Snow depth estimation based on multipath phase combination of GPS triple-frequency signals. *IEEE Trans. Geosci. Remote Sens.* **2015**, *53*, 5100–5109. [CrossRef]
13. Parkinson, B.W.; Enge, P.; Axelrad, P.; Spiker, J., Jr. *Global Positioning System: Theory and Applications*; Author Index; American Institute of Aeronautics and Astronautics, Inc.: Reston, VA, USA, 1996; Volume II, Chapter/Section 10.2; p. 625.

14. Olspert, N.; Pelt, J.; Käpylä, M.J.; Lehtinen, J. Estimating activity cycles with probabilistic methods-I. Bayesian generalised Lomb-Scargle periodogram with trend. *Astron. Astrophys.* **2018**, *615*, A111. [CrossRef]
15. Larson, K.M.; Lay, T.; Yamazaki, Y.; Cheung, K.F.; Ye, L.; Williams, S.D.P.; Davis, J.L. Dynamic sea level variation from GNSS: 2020 Shumagin earthquake tsunami resonance and Hurricane Laura. *Geophys. Res. Lett.* **2021**, *48*, 1378. [CrossRef]